Journal of Nuclear Materials 389 (2009) 115–118

Contents lists available at ScienceDirect

Journal of Nuclear Materials

journal homepage: www.elsevier.com/locate/jnucmat

Thermal and mechanical properties of $(U,Er)O_2$

Shinsuke Yamanaka [a], Ken Kurosaki [a,*], Masahito Katayama [a], Jun Adachi [a], Masayoshi Uno [a], Takeshi Kuroishi [b], Masatoshi Yamasaki [b]

[a] Graduate School of Engineering, Osaka University, 2-1 Yamadaoka, Suita Osaka 565-0871, Japan
[b] Nuclear Fuel Industries Ltd., 1-950, Asashiro-Nishi, Kumatori-cho, Sennan-gun, Osaka 590-0481, Japan

A B S T R A C T

Erbium is considered as a slow burnable poison suitable for use in light water reactors (LWRs). Addition of a small amount of Er_2O_3 to all UO_2 pellets will make it possible to develop super high burnup fuels in Japanese nuclear facilities which are now under the restriction of the upper limit of ^{235}U enrichment. When utilizing the $(U,Er)O_2$ fuels, it is very important to understand the thermal and mechanical properties. Here we show the characterization results of $(U_{1-x}Er_x)O_2$ $(0 \leqslant x \leqslant 0.1)$. We measured their thermal and mechanical properties and investigated the effect of Er addition on these properties of $(U,Er)O_2$. All Er completely dissolved in UO_2, and the lattice parameter decreased linearly with the Er content. Both the thermal conductivity and Young's modulus of $(U,Er)O_2$ decreased with the Er content. These results would be useful for us in evaluating the performance of the $(U,Er)O_2$ fuels in LWRs.

1. Introduction

In order to reduce the amount of spent fuel of nuclear power plants, it is effective to develop super high burnup fuels with higher enrichment of ^{235}U than the current limit criteria of 5 wt%. However, the Japanese nuclear facilities are restricted by law to remain below this upper limit of fuel enrichment for safety reasons. In such a situation, by adding small amounts of erbia (Er_2O_3) to all the uranium dioxide (UO_2) powders whose enrichment is more than 5 wt%, the super high burnup will be achieved with maintaining the criticality safety of the nuclear facilities, because the critical safety of the Er-doped UO_2 fuels will be equivalent to the UO_2 fuels with enrichment of 5 wt% or less. We call this concept 'Erbia Credit', in which Er would play a role as a slow burnable poison suitable for use in light water reactors (LWRs).

In order to utilize the Er-doped UO_2 fuels, it is important to understand basic physical properties of the fuels. Our group has performed the thermal and mechanical characterizations of the Er-doped UO_2 fuel pellets.

In the present paper, we will show the characterization results of the Er-doped UO_2 fuel pellets. We prepared high density fuel pellets with various Er contents up to 10 at.%, and performed the thermal and mechanical characterizations. We revealed the effect of the Er content on the physical properties of $(U,Er)O_2$.

2. Experiment

We prepared nine compositions of the fuel pellets: $(U_{1-x}Er_x)O_2$ ($x = 0$, 0.0028, 0.0056, 0.01, 0.0141, 0.03, 0.05, 0.083, and 0.1). Appropriate amounts of UO_2 and Er_2O_3 powders were mixed and pressed into pellets, followed by reacting at 1773 K under a reducing atmosphere. The obtained intermediates were crushed to powders and pressed into pellets under 150 MPa followed by sintering at 1873 K in a H_2–Ar gas flow atmosphere for 5 h. Finally, the pellets were sintered again at 1373 K in a desired reducing atmosphere for 40 h to fix the oxygen to metal (O/M) ratio to be 2.00.

To examine the phase equilibria and determine the lattice parameter, we collected powder X-ray diffraction (XRD) data on a diffractometer (RINT2000, RIGAKU) with Cu Kα radiation in air at room temperature. The sample microstructure was observed by using a scanning electron microscope (SEM) and electron backscatter diffraction (EBSD). The chemical composition of the samples was determined using an energy-dispersive X-ray (EDX) analysis. The sample density was calculated from the sample weight and dimensions at room temperature.

The Young's modulus of the pellets was evaluated from the longitudinal and shear sound velocities measured by an ultrasonic pulse-echo method at room temperature in air. The experimental samples were bonded to a 5 MHz longitudinal or shear sound wave echogenic transducer. The method to evaluate the Young's modulus from the sound velocities was explained in detail elsewhere [1]. The thermal expansion was measured by using a thermal dilatometer from room temperature to 1500 K. The thermal conductivity (λ) was calculated from the heat capacity (C_P), thermal diffusivity (α), and density (d) using the relationship of $\lambda = \alpha C_P d$.

* Corresponding author. Tel.: +81 6 6879 7905; fax: +81 6 6879 7889.
E-mail address: kurosaki@see.eng.osaka-u.ac.jp (K. Kurosaki).

0022-3115/$ - see front matter © 2009 Elsevier B.V. All rights reserved.
doi:10.1016/j.jnucmat.2009.01.016

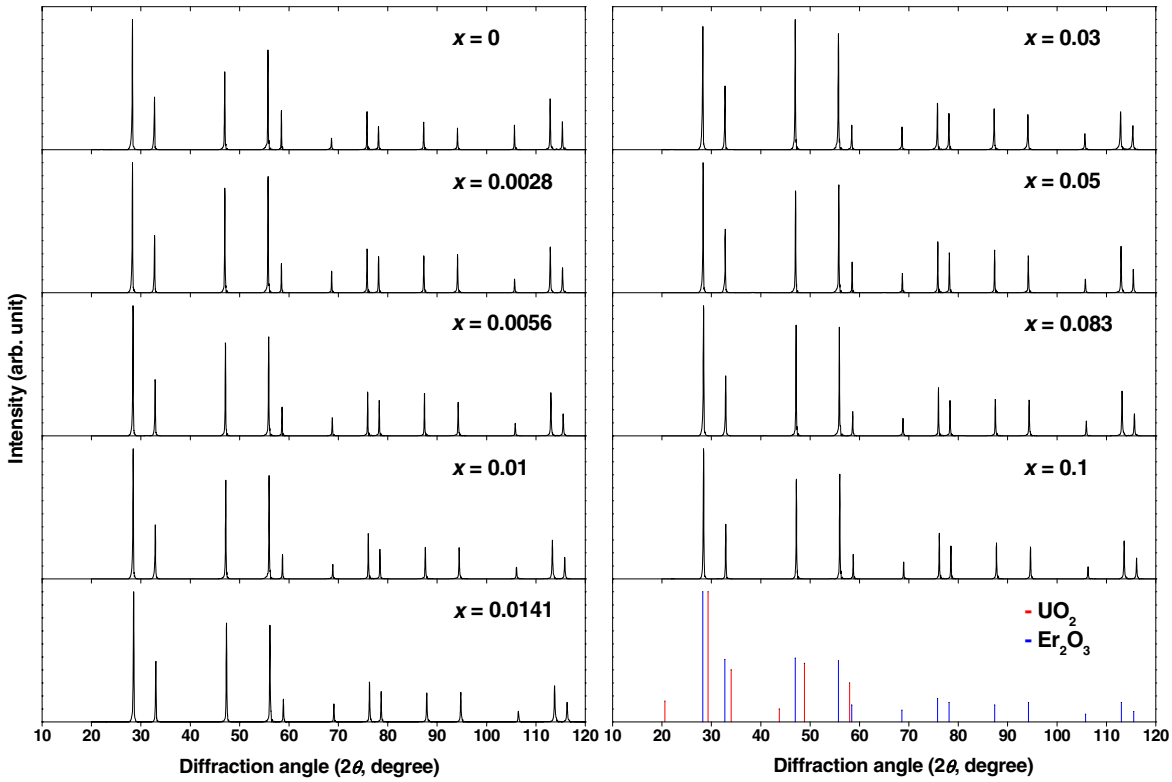

Fig. 1. XRD patterns of Er-doped UO_2: $(U_{1-x}Er_x)O_2$ (x = 0, 0.0028, 0.0056, 0.01, 0.0141, 0.03, 0.05, 0.083, 0.1), together with the peak positions of UO_2 and Er_2O_3.

The heat capacity was measured by a differential scanning calorimeter (DSC), in the temperature range from room temperature to 1500 K in an Ar flow atmosphere. The thermal diffusivity was measured by the laser flash method from room temperature to 1500 K in a vacuum (10^{-4} Pa).

3. Results and discussion

The powder XRD patterns of the pellets are shown in Fig. 1, together with the peak positions of UO_2 and Er_2O_3 derived from the JCPDS cards [2]. In all the XRD patterns, there are no peaks derived from impurities, only the peaks corresponding to the CaF_2 type structure was detected. This means that all Er completely dissolved in UO_2, i.e., we succeeded preparing single phase $(U,Er)O_2$ solid solutions.

From the powder XRD patterns, the cubic lattice parameter was calculated. The calculated lattice parameters were plotted in Fig. 2, as a function of the Er content. In this figure, the literature data reported by Kim et al. [3,4] are also plotted for comparison. Our data as well as the literature data of the lattice parameter linearly decreased with increasing the Er content. However, the lattice parameters obtained here were slightly lower than those of the literature data. This fact can be explained by the difference of the O/M ratio of the pellets.

The pellet densities calculated from the weight and dimensions are plotted in Fig. 3, as a function of the Er content. In the very low

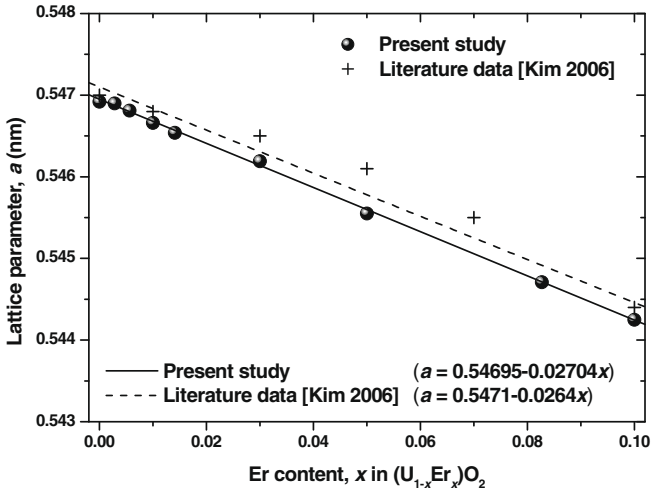

Fig. 2. Lattice parameters of $(U,Er)O_2$, as a function of the Er content.

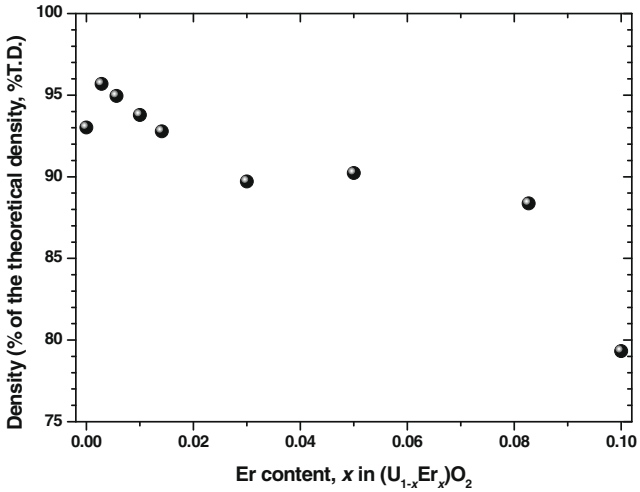

Fig. 3. Bulk densities of the $(U,Er)O_2$ pellets, as a function of the Er content.

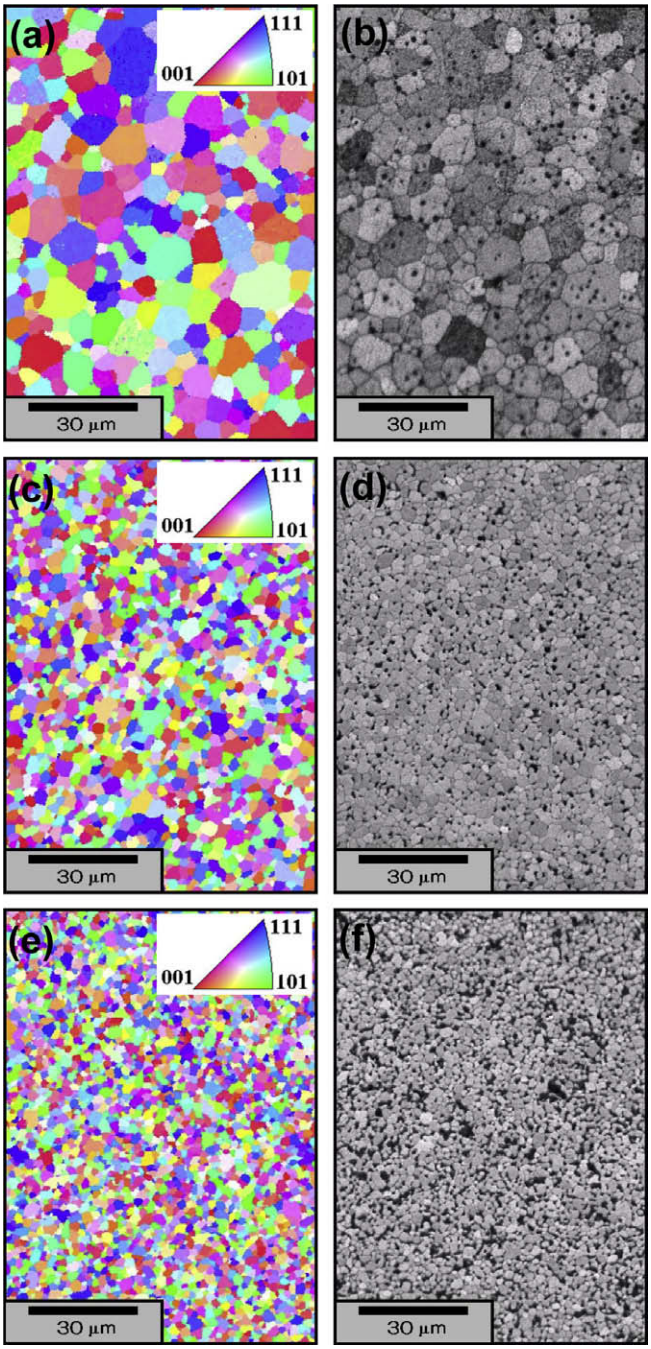

Fig. 4. Inverse pole figure (IPF) and image quality (IQ) mapping results of the $(U_{1-x}Er_x)O_2$ pellets obtained from the EBSD analysis. (a) and (b): IPF and IQ maps for $x = 0.0028$; (c) and (d): IPF and IQ maps for $x = 0.03$; (e) and (f): IPF and IQ maps for $x = 0.1$.

Er content region below 1 at.%, we were able to obtain high density pellets with around 95% of the theoretical density (%T.D.), whereas in the medium Er content region, i.e., 3, 5, and 8.3 at.%, the densities were around 90%T.D. And finally, the density of the 10 at.% Er-doped UO_2 pellet was only 78%T.D. These characteristics could be understood from the viewpoint of the grain size. The inverse pole figure (IPF) and image quality (IQ) mapping results of the $(U,Er)O_2$ pellets obtained from the EBSD analysis are shown in Fig. 4. The grain size seems to decrease with the Er content, which probably led to the low pellet density. Unfortunately, the reason of the grain size decrease was not clear. Nevertheless, the present

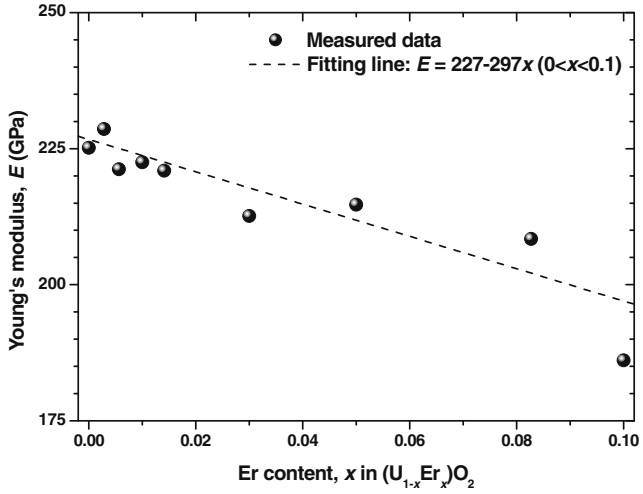

Fig. 5. Young's modulus of the $(U,Er)O_2$ pellets, as a function of the Er content.

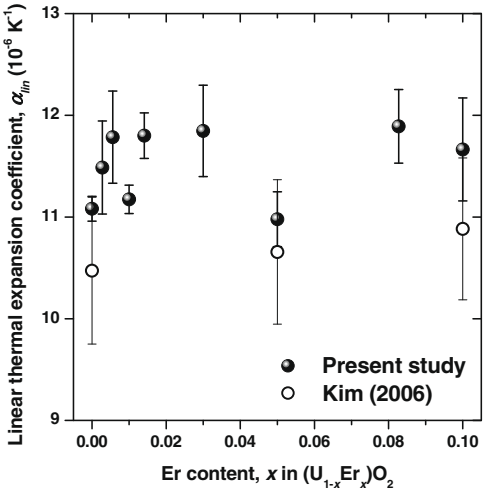

Fig. 6. Average linear thermal expansion coefficient in the temperature range of 323–1373 K of the $(U,Er)O_2$ pellets, measured by using the dilatometer.

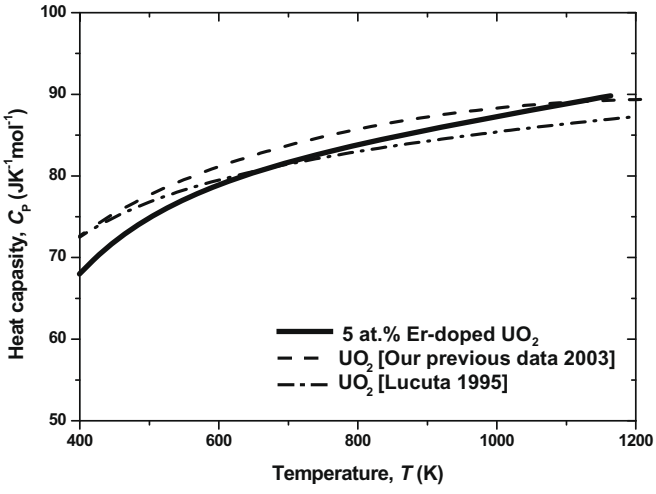

Fig. 7. Temperature dependence of the heat capacity of 5 at.% Er-doped UO_2, together with the data of UO_2.

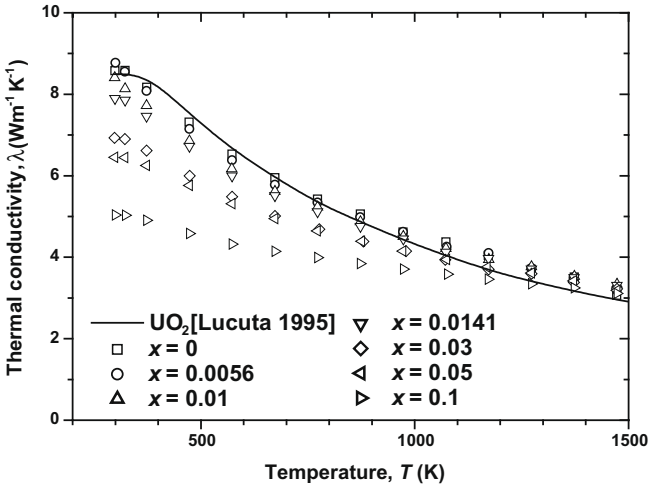

Fig. 8. Temperature dependence of the thermal conductivities of the $(U,Er)O_2$ pellets, together with the data of UO_2.

study revealed that a small amount of Er addition to UO_2 even only a few percent encumbered the grain growth and consequently drastically degenerated the sintering behavior.

The values of the Young's modulus of the $(U,Er)O_2$ pellets are shown in Fig. 5, as a function of the Er content. These values were corrected to the values for fully dense pellets with 100%T.D. The Young's modulus of UO_2 was 227 GPa, well corresponding to the literature data [5], and it decreased with the Er content.

The average linear thermal expansion coefficients in the temperature range from 323 K to 1373 K of the $(U,Er)O_2$ pellets are shown in Fig. 6. The thermal expansion was measured with the dilatometer for rectangular-shaped samples sliced from the pellets. There were no systematic variations with the Er content in the thermal expansion behavior of the $(U,Er)O_2$ pellets. The average linear thermal expansion coefficient of $(U,Er)O_2$ was almost constant independent of the Er content and the values were 11–12 $\times 10^{-6}\,K^{-1}$, which was slightly higher than that of pure UO_2.

The temperature dependence of the heat capacity of 5 at.% Er-doped UO_2 is shown in Fig. 7, together with the data of pure UO_2 [6,7]. The heat capacity data of the Er-doped UO_2 were similar to those of UO_2. The present study revealed that the heat capacities of $(U,Er)O_2$ were scarcely affected by Er-adding.

The temperature dependence of the thermal conductivity of $(U,Er)O_2$ is shown in Fig. 8, together with the data of pure UO_2 [6]. These data were corrected to the values for fully dense pellets with 100%T.D. Clearly, the thermal conductivity of $(U,Er)O_2$ decreased with the Er content, indicating that the Er in the UO_2 cell acted as centers of phonon scattering. This characteristic was also confirmed in a similar case, such as Gd-doped UO_2 [8].

4. Summary

We prepared $(U_{1-x}Er_x)O_2$ $(0 \leqslant x \leqslant 0.1)$ pellets and measured their thermal and mechanical properties. We succeeded in evaluating the effect of the Er content on the physical properties of the $(U,Er)O_2$ pellets. We obtained the following empirical equations describing the lattice parameter, the Young's modulus, and the thermal conductivity of $(U_{1-x}Er_x)O_2$, as a function of the Er content, x:

$$a(\mathrm{nm}) = 0.5471 - 0.0364x \ (0 \leqslant x \leqslant 0.1), \tag{1}$$

$$E(\mathrm{GPa}) = 227 - 297x \ (0 \leqslant x \leqslant 0.1), \tag{2}$$

$$\lambda(\mathrm{Wm^{-1}K^{-1}}) = \frac{1}{6.44 \times 10^{-2} + 1.02x + (1.55 - 4.63x) \times 10^{-4} T} \times (0 \leqslant x \leqslant 0.1, 298\mathrm{K} < T < 1473\mathrm{K}). \tag{3}$$

These data would be very useful in evaluating safety and reliability of the Er-doped fuels which could be utilized in an advanced LWRs aimed at realizing high burnups.

References

[1] S. Yamanaka, M. Fujikane, T. Hamaguchi, H. Muta, T. Oyama, T. Matsuda, S. Kobayashi, K. Kurosaki, J. Alloys Compd. 359 (2003) 109.
[2] JCPDS 5-0550 (UO_2), JCPDS 8-0050 (Er_2O_3).
[3] S.-H. Kim, H.-S. Kim, Y.-W. Kim, D.-S. Sohn, D.-S. Suhr, Mater. Lett. 60 (2006) 480.
[4] S.-H. Kim, Y. -Gu Kim, H.-S. Kim, S.-H. Na, Y.-W. Lee, D.-S. Suhr, J. Nucl. Mater. 342 (2005) 119.
[5] D.L. Hagrman, G.A. Reyman, "MATPRO-0ersion 11: A Handbook of Materials Properties for Use in The Analysis of Light Water Reactor Fuel Rod Behavior," NUREG/CR-0497, TREE-1280, Rev. 3, 1979.
[6] P.G. Lucuta, H. Matzke, R.A. Verrall, J. Nucl. Mater. 223 (1995) 51.
[7] Y. Saito, Thermal and Mechanical Properties of High-Burnup SIMFUEL, Master Thesis, Osaka University, Japan, 2003.
[8] M. Hirai, S. Ishimoto, J. Nucl. Sci. Technol. 28 (1991) 995.